

Design of an Electromagnetic Calorimeter for use at a future e^+e^- Linear Collider

J. S. Marshall^{a,*}

^aCavendish Laboratory, University of Cambridge, Cambridge, United Kingdom

Abstract

Lorem ipsum dolor sit amet, consectetur adipiscing elit, sed diam nonummy nibh euismod tincidunt ut laoreet dolore magna aliquam erat volutpat. Ut wisi enim ad minim veniam, quis nostrud exerci tation ullamcorper suscipit lobortis nisl ut aliquip ex ea commodo consequat. Duis autem vel eum iriure dolor in hendrerit in vulputate velit esse molestie consequat, vel illum dolore eu feugiat nulla facilisis at vero eros et accumsan et iusto odio dignissim qui blandit praesent luptatum zzril delenit augue duis dolore te feugait nulla facilisi. Nam liber tempor cum soluta nobis eleifend option congue nihil imperdiet doming id quod mazim placerat facer possim assum. Typi non habent claritatem insitam; est usus legentis in iis qui facit eorum claritatem. Investigationes demonstraverunt lectores legere me lius quod ii legunt saepius. Claritas est etiam processus dynamicus, qui sequitur mutationem consuetudium lectorum. Mirum est notare quam littera gothica, quam nunc putamus parum claram, anteposuerit litterarum formas humanitatis per seacula quarta decima et quinta decima. Eodem modo typi, qui nunc nobis videntur parum clari, fiant sollemnes in futurum.

Keywords: Particle flow calorimetry, ECAL, Linear Collider, CLIC

1. Introduction

1 Lorem ipsum dolor sit amet, consectetur adipiscing
2 elit, sed diam nonummy nibh euismod tincidunt ut
3 laoreet dolore magna aliquam erat volutpat. Ut wisi
4 enim ad minim veniam, quis nostrud exerci tation
5 ullamcorper suscipit lobortis nisl ut aliquip ex ea
6 commodo consequat. Duis autem vel eum iriure dolor in
7 hendrerit in vulputate velit esse molestie consequat, vel
8 illum dolore eu feugiat nulla facilisis at vero eros et
9 accumsan et iusto odio dignissim qui blandit praesent
10 luptatum zzril delenit augue duis dolore te feugait nulla
11 facilisi. Nam liber tempor cum soluta nobis eleifend
12 option congue nihil imperdiet doming id quod mazim plac-
13 erat facer possim assum. Typi non habent claritatem
14 insitam; est usus legentis in iis qui facit eorum claritatem.
15 Investigationes demonstraverunt lectores legere me lius
16 quod ii legunt saepius. Claritas est etiam processus dy-
17 namicus, qui sequitur mutationem consuetudium lecto-
18 rum. Mirum est notare quam littera gothica, quam nunc
19 putamus parum claram, anteposuerit litterarum formas
20 humanitatis per seacula quarta decima et quinta decima.

22 Eodem modo typi, qui nunc nobis videntur parum clari,
23 fiant sollemnes in futurum.

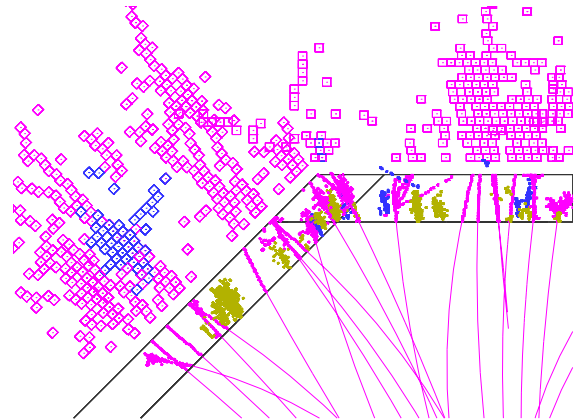


Figure 1

2. Implementation

2.1. Simulation

25 The simulation of detector model response to var-
26 ious physics events was performed using MOKKA.
27

*Corresponding author
Email address: marshall@hep.phy.cam.ac.uk (J. S. Marshall)

28 MOKKA uses Geant4 and the geometry information for
 29 a given detector model to produce detailed simulations
 30 of detector response for various ILC detector concepts.
 31 The flexibility in MOKKA allows various detector pa-
 32 rameters to be modified and so optimisation studies can
 33 be performed. In this study the optimisation was per-
 34 formed with respect to the ILD detector model.

35 2.2. Reconstruction

36 The reconstruction of physics events was performed
 37 using the MARLIN reconstruction framework, which
 38 allows for modular implementation of various c++ pro-
 39 grams each tasked with one aspect of the reconstruc-
 40 tion. While several programs are used in the full recon-
 41 struction it is important to highlight firstly to the pattern
 42 recognition implementation of particle flow calorime-
 43 try, which is done using PandoraPFA, and secondly the
 44 digitisation of calorimeter hits, implemented in the ILD-
 45 CaloDigi processor.

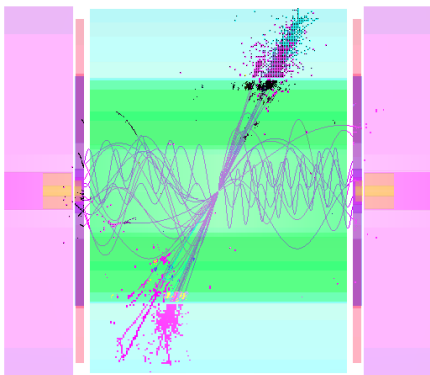


Figure 2: Typical topologies 250GeV jets simulated in the ILD detector model.

46 2.2.1. PandoraPFA

47 The PandoraPFA software package implements the
 48 pattern recognition side of particle flow calorimetry. It
 49 is essential that calorimeter hits are correctly assigned
 50 to charged particle tracks to avoid double counting of
 51 energy in the particle flow paradigm. This can be ex-
 52 tremely challenging given the complex topologies asso-
 53 ciated to particle showers at high energies such as those
 54 shown in figure 2.

55 Due to the varied nature of detector models be-
 56 ing simulated in these studies it is necessary to have
 57 reusable and flexible software that is isolated from the
 58 detector model. This is achieved using the Pandora
 59 Software Development Kit (PandoraSDK), which is an

60 independent framework for applying sophisticated topo-
 61 logical algorithms designed to perform the association
 62 of calorimeter hits to charged particle tracks. The al-
 63 gorithm logic applied in PandoraSDK is independent of
 64 detector model.

65 2.2.2. ILDCaloDigi

66 The ILDCaloDigi processor is designed to perform
 67 the digitisation of calorimeter hits for the ILD detector
 68 model. Digitisation of calorimeter hits is the process by
 69 which the energy deposits in the absorber (non-active)
 70 region of a calorimeter cell is estimated using the mea-
 71 sured value of the energy deposited in the active region
 72 of the cell. Accurate energy estimators for calorimeter
 73 cells is crucial for estimating detector performance and
 74 so calibration at this stage is essential for all simula-
 75 tions.

76 A number of realistic effects can be simulated using
 77 the ILDCaloDigi processor, the full details of which can
 78 be found here. For these studies electrical noise and a
 79 limited electronics read out range was simulated and the
 80 effect of timing cuts was analysed in detail.

81 2.3. Calibration

82 To ensure reliability in the conclusions drawn from
 83 these optimisation studies, it was necessary to calibrate
 84 the response of each detector model considered. This
 85 occurred in three stages, the full details of which can be
 86 found here.

87 Initially, the detector response to minimum ionising
 88 particles (MIPs) was determined by looking at the de-
 89 tector response to muons. This set the MIP scale in both
 90 the digitiser and inside PandoraPFA, which is needed as
 91 a reference energy unit for applying thresholds and cuts.

92 Secondly, the digitisation stage of the reconstruction
 93 was tuned for events of photons and long lived neutral
 94 kaons for events that were contained within the ECAL
 95 and HCAL respectively. This tuning was an iterative
 96 procedure where constants in the digitisation proces-
 97 sor, ILDCaloDigi, were varied and simulations repeated
 98 until the sum of calorimeter hit energies matched the
 99 Monte-Carlo energy of the photons and long lived neu-
 100 tral kaons being simulated.

101 Finally, the electromagnetic and hadronic energy
 102 scales within PandoraPFA must be correctly set. This
 103 is done by independently scaling the energy of parti-
 104 cle flow objects (PFOs), the output reconstructed parti-
 105 cles from PandoraPFA, for PFOs originating from elec-
 106 tron magnetic and hadronic showers separately. This is
 107 again done in an iterative procedure involving changing
 108 the inputs to PandoraPFA and repeating simulations un-
 109 til the PFO energy matches the Monte-Carlo energy for

110 the photons (electromagnetic showers) and long lived
 111 neutral kaons (hadronic showers) being simulated.

112 2.4. Parameterising Detector Performance

113 The primary figure of merit used in these optimisation
 114 studies is the jet energy resolution, as extensively
 115 described in (Pandora paper chapter 5). The jets used
 116 in these studies are from the decay of off-shell mass Z
 117 bosons decaying at rest into a pair of light quarks (u,d,s).
 118 Typically, such decays form mono-energetic jets back to
 119 back as can be seen in figure 2.

120 Detector performance, in the particle flow paradigm,
 121 is a combination of intrinsic energy resolution and pat-
 122 tern recognition. It is possible to isolate the magnitude
 123 of these two contributions to the jet energy resolution
 124 by cheating the pattern reconstruction using the Monte
 125 Carlo (MC) information, as shown in figure 3. Analy-
 126 sis of this information extends understanding of the
 127 behaviour of a detector model and will be beneficial for
 128 detector model comparisons.

129 A reconstruction where the pattern recognition is
 130 fully cheated provides the intrinsic energy resolution
 131 contribution to the jet energy resolution. The quadrature
 132 difference between the default reconstruction jet energy
 133 resolution, which uses no MC information, and the fully
 134 cheated reconstruction jet energy resolution provides
 135 the confusion contribution to the jet energy resolution.
 136 This confusion term arises due to the misidentification
 137 of the origin of some energy deposits in the detector.

138 By only cheating certain aspects of the reconstruc-
 139 tion, it is possible to decompose the confusion into
 140 terms related to the misidentification of energy deposits
 141 from certain classes of particles such as photons or neu-
 142 tral hadrons. Figure 4 shows a typical example of this
 143 decomposition where the photon and neutral hadron
 144 confusions have been isolated. The other confusion is
 145 the quadrature difference between the total confusion
 146 and the sum of the photon and neutral hadron confu-
 147 sions.

148 3. Default Detector Performance

149 In these studies the reference detector model will be
 150 the ILD detector model. In this model the ECal consists
 151 of a 30 layer, silicon-tungsten ECal with a square cell
 152 size of $5 \times 5\text{mm}^2$ containing ~ 24 radiation lengths (X_0)
 153 and ~ 1 nuclear interaction length (λ_I). The HCal con-
 154 sists of a 48 layer, scintillator-steel HCal with a square
 155 cell size of $30 \times 30\text{mm}^2$ containing $\sim 50X_0$ and $\sim 6\lambda_I$.

156 In order to have confidence in the conclusions drawn
 157 from detector model comparisons, a number of parame-
 158 ters used in the reconstruction should be specified. Both

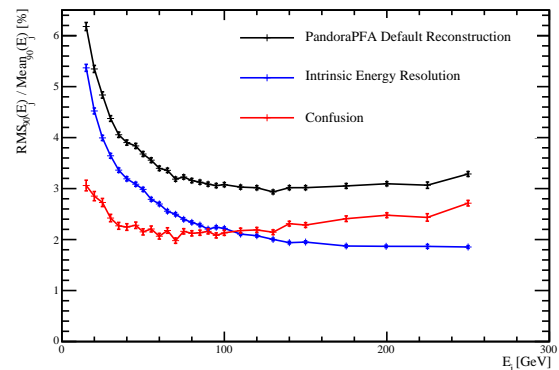


Figure 3: Jet energy resolution as a function of jet energy for the ILD detector model. The jet energy resolution has been decomposed into the intrinsic energy resolution and the confusion terms.

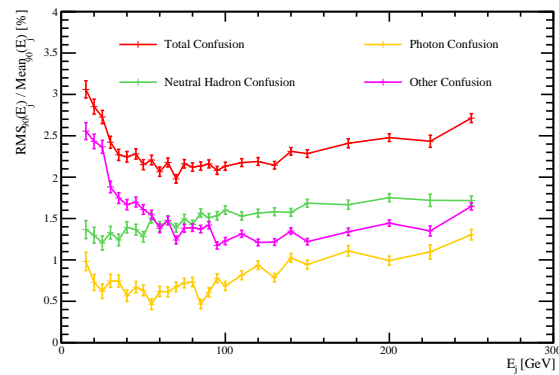


Figure 4: Confusion decomposed into various terms as a function of jet energy. Simulation was performed using the ILD detector model.

159 the timing cut placed on the simulation and the hadronic
 160 energy truncation applied to digitised HCal cells in Pan-
 161 draPFA have a large impact on the detector perfor-
 162 mance. The details of their dependency of detector per-
 163 formance is described in sections 3.1 and 3.2.

164 For these studies the default jet energy resolutions are
 165 shown in table 1.

166 3.1. Timing Cuts

167 When considering calorimetry at a collider exper-
 168 iment, a balance has to be struck between allowing
 169 enough time for particle showers to develop and reading
 170 out signals, integrated over multiple collisions, at a suf-
 171 ficiently fast rate to prevent saturation. Therefore, hits
 172 in the calorimeter after a time of $O(100\text{ns})$ corrected
 173 for time of flight will not be used in the reconstruction.

Jet Energy (GeV)	rms (GeV)	$\text{rms}_{90}(E_{jj})$ (GeV)	$\text{rms}_{90}(E_j) / E_j$ (%)
45.5	3.32	2.35	(3.68±0.05)
100	7.83	4.08	(2.90±0.04)
180	10.89	7.32	(2.89±0.04)
250	18.18	10.43	(2.98±0.04)

Table 1: Default ILD detector performance. A 100 ns timing cut was applied to this simulation and the hadronic energy truncation applied in PandoraPFA was 1 GeV.

The impact of this timing cut on the reconstruction is shown in figure 5. In the following studies a timing cut of 100ns was applied to all simulations.

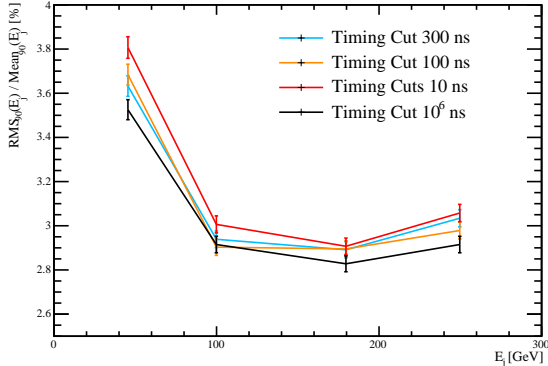


Figure 5: Jet energy resolution as a function of jet energy for the ILD detector model with various timing cuts applied to the reconstruction. The hadronic energy truncation applied to these simulations is 1 GeV.

3.2. Hadronic Energy Truncation

In sampling calorimeters, it is possible to apply software compensation to improve the estimation of energy deposited in the inactive medium of the calorimeters. A simplistic form of software compensation applied in PandoraPFA is truncation, on a per cell basis, of the hadronic energy measured in the HCal. The effect of this software compensation is twofold, firstly, it improves the energy estimators of the particle showers in the calorimeters and, secondly, the improved energy estimators make the pattern recognition logic more effective. Both of these effects can be seen clearly in figure 6, which shows an improvement in both the intrinsic energy resolution of the detector and a reduction in the pattern recognition confusion when a truncation of 1 GeV is applied to the default detector.

The truncation value applied in PandoraPFA strongly determines the performance of the detector. The dependency of detector performance on the hadronic energy truncation can be seen in figure 7. The optimal value of the hadronic energy truncation varies both as a function of jet energy and detector model. The value of the truncation is optimised for each detector model considered in the studies presented here, however, the truncation applied is kept independent of the jet energy.

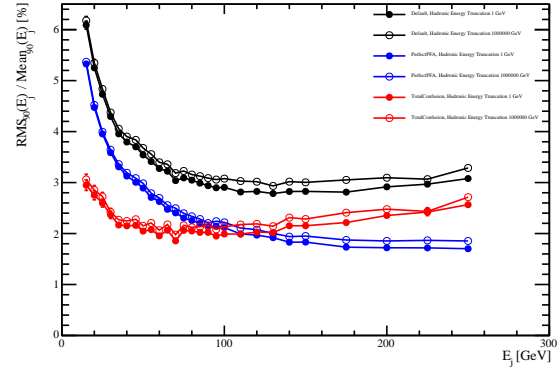


Figure 6: Jet energy resolution as a function of jet energy for the ILD detector model with various timing cuts applied to the reconstruction.

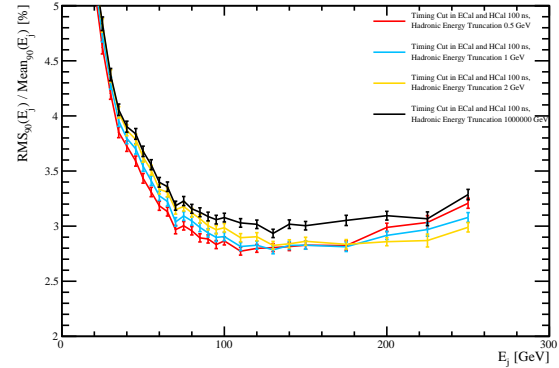


Figure 7: Jet energy resolution as a function of jet energy for the ILD detector model with various timing cuts applied to the reconstruction. The hadronic energy truncation applied to these simulations is 1 GeV.

4. ECAL Parameter Scan

Sampling of electromagnetic particle showers in ILD occurs primarily in the ECAL. Due to the $\sim 24X_0$ contained within the ECAL all but the highest energy electromagnetic showers will be contained within the ECAL.

207 The $\sim 1\lambda_I$ contained in the ECal also means that some
 208 hadronic showers will be forming in the ECal, but
 209 the bulk of the hadronic showers will be found in the
 210 HCal.

211 The ECal requires fine longitudinal and transverse
 212 granularities such that the separation of nearby particle
 213 showers becomes possible via the application of sophis-
 214 ticated pattern recognition algorithms provided by Pan-
 215 dorapfa. For the default ILD ECal, there are 30 layers
 216 and a cell size is $5 \times 5\text{mm}^2$, which does provide suf-
 217 ficient granularity for the application of particle flow
 218 calorimetry. The optimisation of these granularities is
 219 considered in the following chapter.

220 The default detector model uses silicon as the active
 221 material for the ECal. However, using scintillator for the
 222 active material would be a more cost effective option. A
 223 comparison between these two active material choices is
 224 presented below to determine which of the two options
 225 gives the best physics performance.

226 4.1. ECal Active Material

227 The impact of the active material on the intrinsic en-
 228 ergy resolution of the detector can be seen in figure 8.
 229 The energy resolution for the two options is comparable,
 230 but scintillator active material shows a small reduction
 231 in the resolution.

232 Figure 9, which shows a reduction in the misidentifi-
 233 cation of photon energy deposits, the photon confusion,
 234 when silicon is used instead of scintillator as the active
 235 material choice in the ECal. This is to be expected as the
 236 larger Moliere radius in scintillator means electromag-
 237 netic showers are broader, as seen in figure 10, making
 238 pattern recognition more challenging.

239 There is relatively little performance difference when
 240 comparing silicon to scintillator as the ECal absorber
 241 material when considering jet energy resolution, as fig-
 242 ure 10 shows. However, the improved application of
 243 pattern recognition logic for silicon based ECals means
 244 that physics performance for processes where photon
 245 identification is crucial will benefit more from a silicon
 246 based ECal.

247 4.2. Transverse Granularity

248 The dependency of the jet energy resolution on the
 249 ECal cell size is shown in figure 11. As expected the
 250 finer the granularity in the ECal improved the resolution
 251 of the detector. The confusion terms shown in figure
 252 12 clearly show that the improvement in resolution with
 253 a finer granularity ECal is down to a reduction in the
 254 photon confusion.

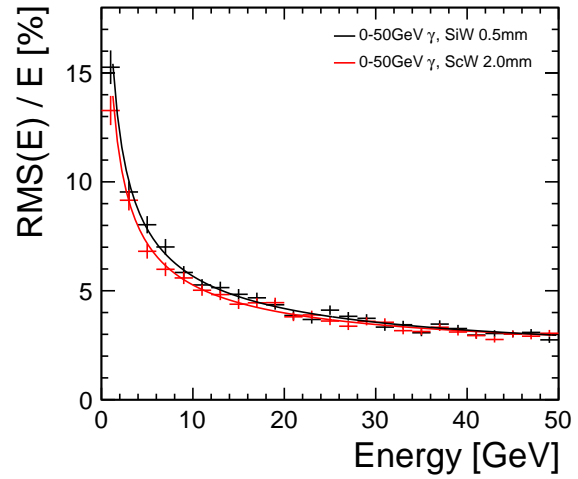


Figure 8: Energy resolution, comparison between scintillator and silicon active materials for the ECal.

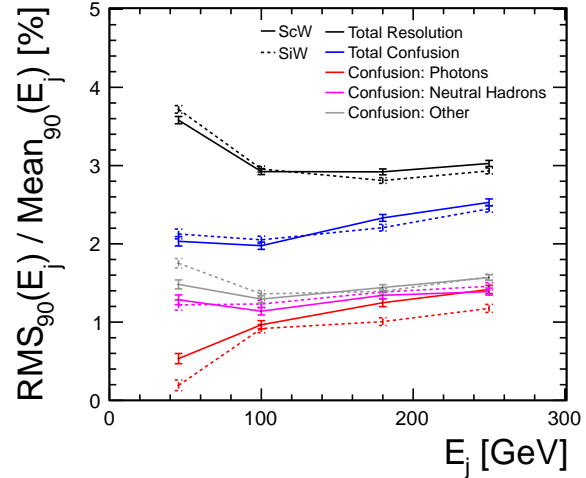


Figure 9: Comparison of the jet energy resolution and the confusion terms as a function of jet energy between silicon and scintillator active material choices for the ECal.

255 4.3. Number of Layers

256 Lorem ipsum dolor sit amet, consectetuer adipisc-
 257 ing elit, sed diam nonummy nibh euismod tincidunt ut
 258 laoreet dolore magna aliquam erat volutpat. Ut wisi
 259 enim ad minim veniam, quis nostrud exerci tation ul-
 260 lamcorper suscipit lobortis nisl ut aliquip ex ea com-
 261 modo consequat. Duis autem vel eum iriure dolor in
 262 hendrerit in vulputate velit esse molestie consequat, vel
 263 illum dolore eu feugiat nulla facilisis at vero eros et ac-
 264 cumsan et iusto odio dignissim qui blandit praesent lup-

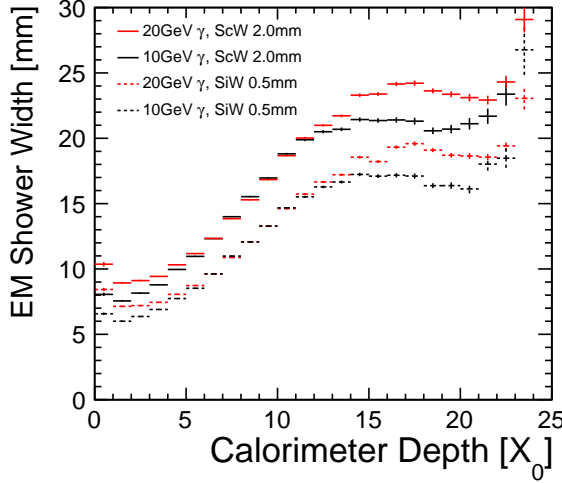


Figure 10: Comparison between the electromagnetic shower widths as a function of layer number when using silicon and scintillator as the active material in the ECal.

tatum zzril delenit augue duis dolore te feugait nulla facilisi. Nam liber tempor cum soluta nobis eleifend option congue nihil imperdiet doming id quod mazim placerat facer possim assum. Typi non habent claritatem insitam; est usus legentis in iis qui facit eorum claritatem. Investigationes demonstraverunt lectores legere me lius quod ii legunt saepius. Claritas est etiam processus dynamicus, qui sequitur mutationem consuetudium lectorum. Mirum est notare quam littera gothica, quam nunc putamus parum claram, anteposuerit litterarum formas humanitatis per seacula quarta decima et quinta decima. Eodem modo typi, qui nunc nobis videntur parum clari, fiant sollemnes in futurum.

5. HCAL Parameter Scan

ILD detector model used. Timing cuts used are 10ns in HCal and 20ns in ECal. No MaxHCalHitHadronicEnergy. Full calibration procedure applied for all detector models. QGSP_BERT physics list used in all cases except Fe and W comparison where both QGSP_BERT and QGSP_BERT_HP used.

5.1. Fe/W HCAL Comparison

The feasible options for HCal absorber material are steel (Iron) and tungsten (WMod). The thicknesses of the scintillator and absorber layers of the HCal were scaled to maintain the total number of nuclear interaction lengths in the HCal. The ratio of scintillator and

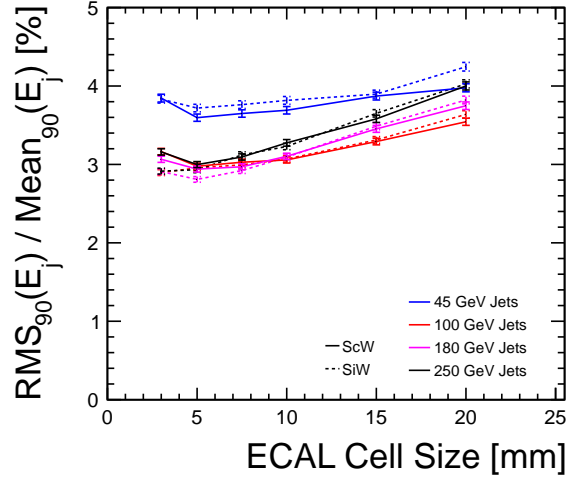


Figure 11: Jet energy resolution as a function of ECal cell size. Results are shown for both silicon and scintillator based ECals at various jet energies.

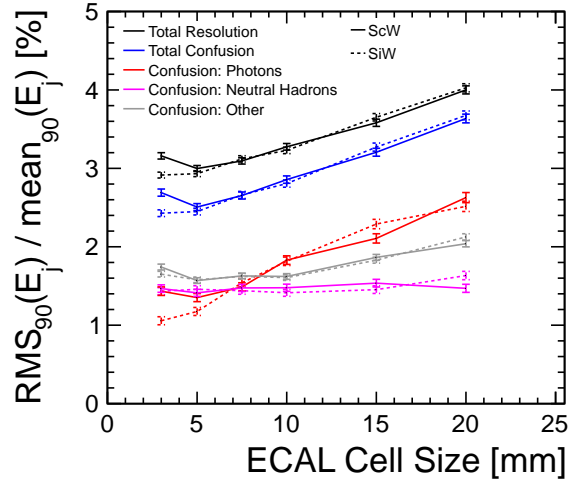


Figure 12: Jet energy resolution and the confusion terms as a function of ECal cell size for 250 GeV jets. Results are shown for both silicon and scintillator based ECals.

Figure 13

absorber thicknesses in the HCal was held constant to maintain the sampling fraction. Otherwise default ILD DBD detector parameters were used.

Both the QGSP_BERT and QGSP_BERT_HP physics lists were used in this analysis. The high precision neutron package, included in QGSP_BERT_HP, offers more realistic modelling of the transportation of neutrons below 20 MeV down to thermal energies. The compact

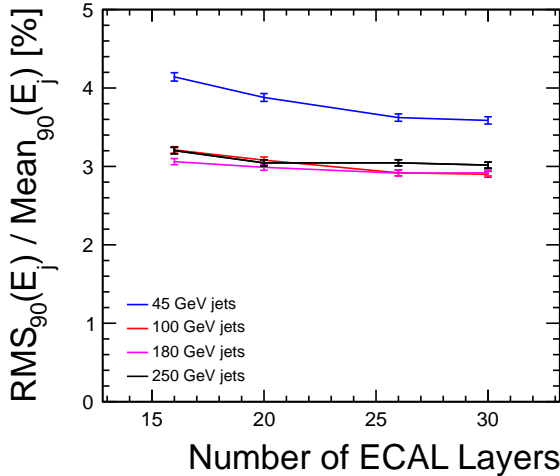


Figure 14: Number Two

299 nature of the hadronic showers showering in tungsten
300 was the primary reason for the inclusion of the high precision
301 neutron package in this analysis.

302 HCals using steel as an absorber material were found
303 to outperform those using tungsten across the entire
304 range of jet energies considered. This trend was found
305 to be more prominent for high energy jets. No strong
306 dependence on the choice of physics list was observed.

307 5.2. Transverse Granularity

308 The transverse granularity of the HCal, the HCal cell
309 size, was varied. Otherwise, default ILD DBD detector
310 parameters were used in this analysis.

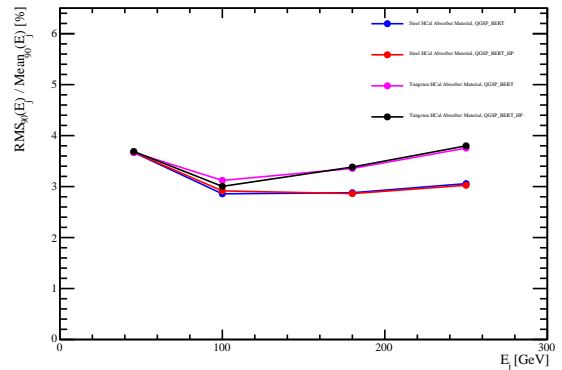


Figure 15: The jet energy resolution as a function of jet energy. Results are shown for detectors using both steel and tungsten HCal absorber materials and using both the QGSP_BERT and QGSP_BERT_HP physics lists.

311 Figure 16 shows the jet energy resolution as a function
312 of HCal cell size for various energy jets. It was
313 found that smaller HCal cell sizes benefited the jet en-
314 ergy resolution and that this trend became more promi-
315 nent for higher energy jets. The jet energy resolution
316 was decomposed into the confusion and intrinsic energy
317 resolution terms. The results of this decomposition for
318 the 250 GeV jets are shown in figure 16.

319 The intrinsic energy resolution was found to be in-
320 variant under changes to HCal cell size. This indicates
321 the performance trend observed for HCal cell size are
322 dictated by the confusion term. This is expected as
323 changes to HCal cell size will aid the association of
324 calorimeter cell clusters to charged particle tracks, but
325 will not affect intrinsic energy resolution.

326 5.3. Number of Layers

327 The number of layers in the HCal was varied. The
328 scintillator and absorber thicknesses were scaled to
329 maintain the total number of nuclear interaction lengths
330 in the HCal. The ratio of scintillator and absorber thick-
331 ness was held constant to maintain the sampling fraction.
332 Otherwise, default ILD DBD detector parameters
333 were used in this analysis.

334 Figure 17 shows the jet energy resolution as a func-
335 tion of the number of layers in the HCal for various en-
336 ergies. It was found that reducing the number of lay-
337 ers in the HCal degrades the jet energy resolution and
338 that this trend applies to all jet energies considered.

339 Insufficient sampling of particle showers in the HCal
340 is likely to be the primary cause of the degradation at
341 low numbers of layers in the HCal.

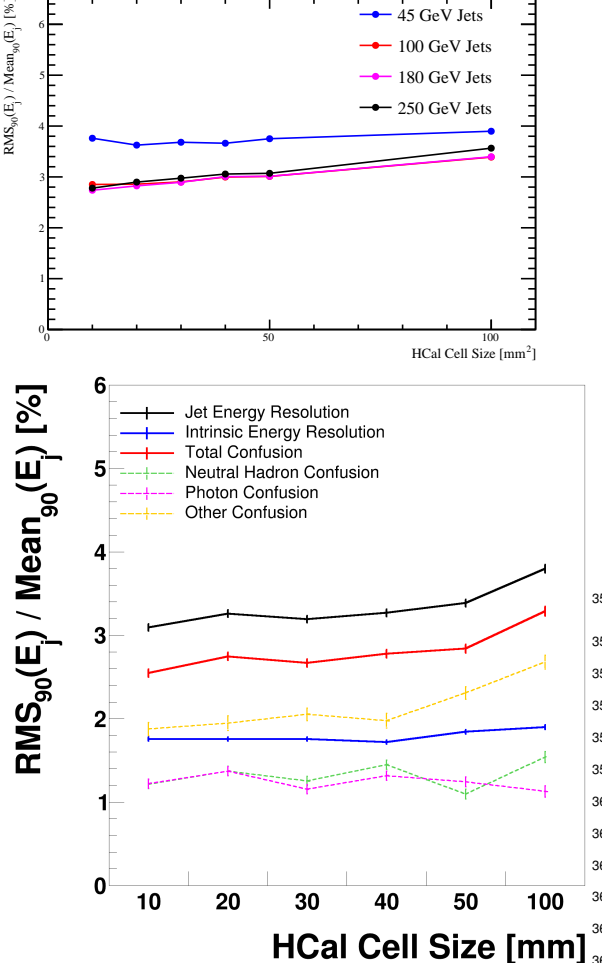


Figure 16: (top) The jet energy resolution as a function of HCal cell size. Results are shown for various jet energies ranging from 45 GeV to 500 GeV. (bottom) The jet energy resolution decomposition as a function of HCal cell size. The results shown are for a jet energy of 250 GeV.

342 5.4. Depth

343 The total number of nuclear interaction lengths in the
 344 HCal was varied by changing both the absorber and
 345 scintillator thicknesses in the HCal. The ratio of absorber
 346 to scintillator thicknesses in the HCal was held
 347 constant to maintain the sampling fraction. Otherwise,
 348 default ILD DBD detector parameters were used in this
 349 analysis.

350 Figure shows the jet energy resolution as a function
 351 of the total number of nuclear interaction lengths in the
 352 HCal. It was found that increasing the number of nu-
 353 clear interaction lengths in the HCal improved the jet

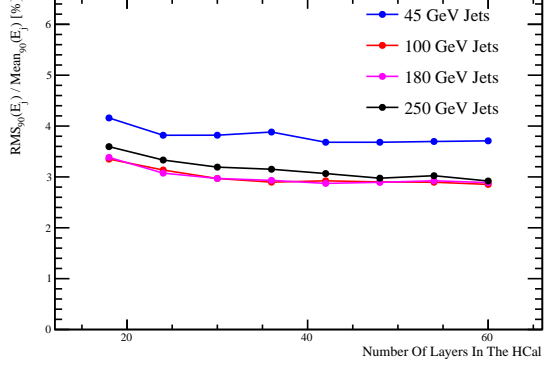


Figure 17: The jet energy resolution as a function of number of layers in the HCal. Results are shown for various jet energies ranging from 45 GeV to 500 GeV.

354 energy resolution for high energy jets.

355 The number of nuclear interaction lengths in the HCal
 356 will determine the impact of leakage of energy out of
 357 the back of the calorimeters. Energy leaked from the
 358 back of the calorimeters will be measured in the muon
 359 chamber. The energy resolution in the muon chamber is
 360 significantly worse than in the calorimeters, therefore,
 361 leakage degrades the jet energy resolution. As jet en-
 362 ergy increases so does the fraction of the total energy
 363 leaking out of the back of the detector. Therefore, re-
 364 ducing leakage is more beneficial to higher energy jets,
 365 which is what is observed.

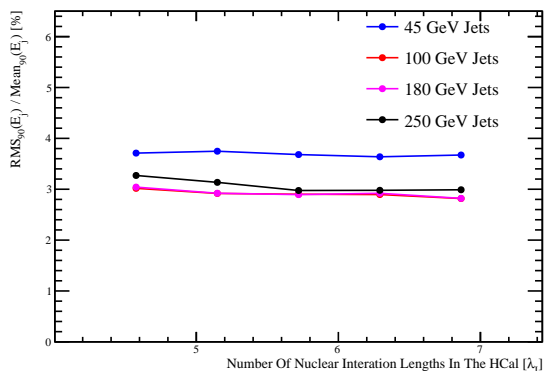


Figure 18: The jet energy resolution as a function of the total number of nuclear interaction lengths in the HCal. Results are shown for various jet energies ranging from 45 GeV to 500 GeV.

366 **5.5. Sampling Fraction in HCal**

367 Sampling fraction varied. Total number of nuclear
 368 interaction lengths in HCal held constant.

369 No picture needed in this section, all jet energy res-
 370 olutions are flat wrt sampling fraction except at 0.05
 371 (range considered 0.05 to 0.25 steps 0.05) where they
 372 start to deteriorate across all jet energies considered.

373 **6. Global Parameter Scan**

374 Lorem ipsum dolor sit amet, consectetur adipisci-
 375 ing elit, sed diam nonummy nibh euismod tincidunt ut
 376 laoreet dolore magna aliquam erat volutpat. Ut wisi
 377 enim ad minim veniam, quis nostrud exerci tation ul-
 378 lamcorper suscipit lobortis nisl ut aliquip ex ea com-
 379 modo consequat. Duis autem vel eum iriure dolor in
 380 hendrerit in vulputate velit esse molestie consequat, vel
 381 illum dolore eu feugiat nulla facilisis at vero eros et ac-
 382 cumsan et iusto odio dignissim qui blandit praesent lup-
 383 tatum zzril delenit augue duis dolore te feugait nulla fa-
 384 cilisi. Nam liber tempor cum soluta nobis eleifend op-
 385 tion congue nihil imperdier doming id quod mazim plac-
 386 erat facer possim assum. Typi non habent claritatem in-
 387 sitam; est usus legentis in iis qui facit eorum claritatem.
 388 Investigationes demonstraverunt lectores legere me lius
 389 quod ii legunt saepius. Claritas est etiam processus dy-
 390 namicus, qui sequitur mutationem consuetudium lecto-
 391 rum. Mirum est notare quam littera gothica, quam nunc
 392 putamus parum claram, anteposuerit litterarum formas
 393 humanitatis per seacula quarta decima et quinta decima.
 394 Eodem modo typi, qui nunc nobis videntur parum clari,
 395 fiant sollemnes in futurum.

396 **6.1. Inner Radius**

397 Lorem ipsum dolor sit amet, consectetur adipisci-
 398 ing elit, sed diam nonummy nibh euismod tincidunt ut
 399 laoreet dolore magna aliquam erat volutpat. Ut wisi
 400 enim ad minim veniam, quis nostrud exerci tation ul-
 401 lamcorper suscipit lobortis nisl ut aliquip ex ea com-
 402 modo consequat. Duis autem vel eum iriure dolor in
 403 hendrerit in vulputate velit esse molestie consequat, vel
 404 illum dolore eu feugiat nulla facilisis at vero eros et ac-
 405 cumsan et iusto odio dignissim qui blandit praesent lup-
 406 tatum zzril delenit augue duis dolore te feugait nulla fa-
 407 cilisi. Nam liber tempor cum soluta nobis eleifend op-
 408 tion congue nihil imperdier doming id quod mazim plac-
 409 erat facer possim assum. Typi non habent claritatem in-
 410 sitam; est usus legentis in iis qui facit eorum claritatem.
 411 Investigationes demonstraverunt lectores legere me lius
 412 quod ii legunt saepius. Claritas est etiam processus dy-
 413 namicus, qui sequitur mutationem consuetudium lecto-
 414 rum. Mirum est notare quam littera gothica, quam nunc

415 putamus parum claram, anteposuerit litterarum formas
 416 humanitatis per seacula quarta decima et quinta decima.
 417 Eodem modo typi, qui nunc nobis videntur parum clari,
 418 fiant sollemnes in futurum.

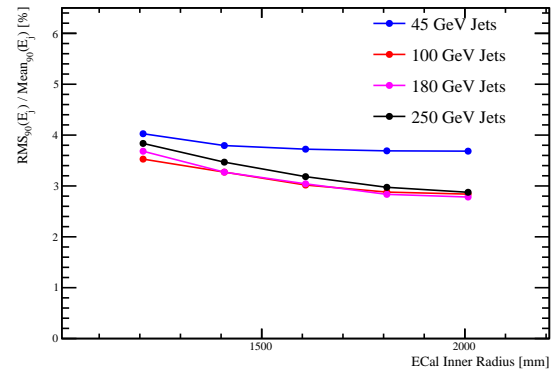


Figure 19: The jet energy resolution as a function of the outer TPC radius. The outer TPC radius can be interpreted as the inner ECal radius. Results are shown for various jet energies ranging from 45 GeV to 500 GeV.

419 **6.2. B-Field Strength**

420 Lorem ipsum dolor sit amet, consectetur adipisci-
 421 ing elit, sed diam nonummy nibh euismod tincidunt ut
 422 laoreet dolore magna aliquam erat volutpat. Ut wisi
 423 enim ad minim veniam, quis nostrud exerci tation ul-
 424 lamcorper suscipit lobortis nisl ut aliquip ex ea com-
 425 modo consequat. Duis autem vel eum iriure dolor in
 426 hendrerit in vulputate velit esse molestie consequat, vel
 427 illum dolore eu feugiat nulla facilisis at vero eros et ac-
 428 cumsan et iusto odio dignissim qui blandit praesent lup-
 429 tatum zzril delenit augue duis dolore te feugait nulla fa-
 430 cilisi. Nam liber tempor cum soluta nobis eleifend op-
 431 tion congue nihil imperdier doming id quod mazim plac-
 432 erat facer possim assum. Typi non habent claritatem in-
 433 sitam; est usus legentis in iis qui facit eorum claritatem.
 434 Investigationes demonstraverunt lectores legere me lius
 435 quod ii legunt saepius. Claritas est etiam processus dy-
 436 namicus, qui sequitur mutationem consuetudium lecto-
 437 rum. Mirum est notare quam littera gothica, quam nunc
 438 putamus parum claram, anteposuerit litterarum formas
 439 humanitatis per seacula quarta decima et quinta decima.
 440 Eodem modo typi, qui nunc nobis videntur parum clari,
 441 fiant sollemnes in futurum.

442 **6.3. Scintillator Thickness**

443 Lorem ipsum dolor sit amet, consectetur adipisci-
 444 ing elit, sed diam nonummy nibh euismod tincidunt ut

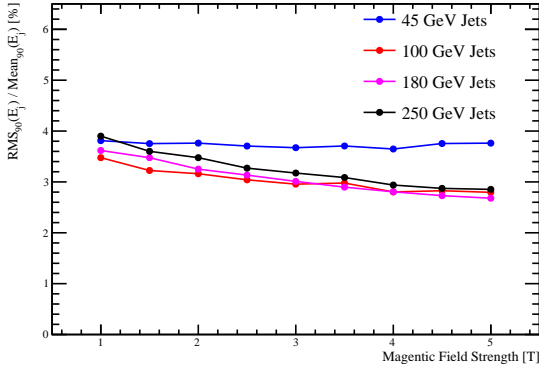


Figure 20: The jet energy resolution as a function of the magnetic field strength within the detector. Results are shown for various jet energies ranging from 45 GeV to 500 GeV.

laoreet dolore magna aliquam erat volutpat. Ut wisi enim ad minim veniam, quis nostrud exerci tation ullamcorper suscipit lobortis nisl ut aliquip ex ea commodo consequat. Duis autem vel eum iriure dolor in hendrerit in vulputate velit esse molestie consequat, vel illum dolore eu feugiat nulla facilisis at vero eros et accumsan et iusto odio dignissim qui blandit praesent luptatum zzril delenit augue duis dolore te feugait nulla facilisi. Nam liber tempor cum soluta nobis eleifend option congue nihil imperdiet doming id quod mazim plac erat facer possim assum. Typi non habent claritatem insitam; est usus legentis in iis qui facit eorum claritatem. Investigationes demonstraverunt lectores legere me lius quod ii legunt saepius. Claritas est etiam processus dynamicus, qui sequitur mutationem consuetudium lectorum. Mirum est notare quam littera gothica, quam nunc putamus parum claram, anteposuerit litterarum formas humanitatis per seacula quarta decima et quinta decima. Eodem modo typi, qui nunc nobis videntur parum clari, fiant sollemnes in futurum.

6.4. Parameterisation of Results

Lorem ipsum dolor sit amet, consectetuer adipisc ing elit, sed diam nonummy nibh euismod tincidunt ut laoreet dolore magna aliquam erat volutpat. Ut wisi enim ad minim veniam, quis nostrud exerci tation ullamcorper suscipit lobortis nisl ut aliquip ex ea commodo consequat. Duis autem vel eum iriure dolor in hendrerit in vulputate velit esse molestie consequat, vel illum dolore eu feugiat nulla facilisis at vero eros et accumsan et iusto odio dignissim qui blandit praesent luptatum zzril delenit augue duis dolore te feugait nulla facilisi. Nam liber tempor cum soluta nobis eleifend op-

tion congue nihil imperdiet doming id quod mazim plac erat facer possim assum. Typi non habent claritatem insitam; est usus legentis in iis qui facit eorum claritatem. Investigationes demonstraverunt lectores legere me lius quod ii legunt saepius. Claritas est etiam processus dynamicus, qui sequitur mutationem consuetudium lectorum. Mirum est notare quam littera gothica, quam nunc putamus parum claram, anteposuerit litterarum formas humanitatis per seacula quarta decima et quinta decima. Eodem modo typi, qui nunc nobis videntur parum clari, fiant sollemnes in futurum.

7. Novel ECAL Models

Lorem ipsum dolor sit amet, consectetuer adipisc ing elit, sed diam nonummy nibh euismod tincidunt ut laoreet dolore magna aliquam erat volutpat. Ut wisi enim ad minim veniam, quis nostrud exerci tation ullamcorper suscipit lobortis nisl ut aliquip ex ea commodo consequat. Duis autem vel eum iriure dolor in hendrerit in vulputate velit esse molestie consequat, vel illum dolore eu feugiat nulla facilisis at vero eros et accumsan et iusto odio dignissim qui blandit praesent luptatum zzril delenit augue duis dolore te feugait nulla facilisi. Nam liber tempor cum soluta nobis eleifend option congue nihil imperdiet doming id quod mazim plac erat facer possim assum. Typi non habent claritatem insitam; est usus legentis in iis qui facit eorum claritatem. Investigationes demonstraverunt lectores legere me lius quod ii legunt saepius. Claritas est etiam processus dynamicus, qui sequitur mutationem consuetudium lectorum. Mirum est notare quam littera gothica, quam nunc putamus parum claram, anteposuerit litterarum formas humanitatis per seacula quarta decima et quinta decima. Eodem modo typi, qui nunc nobis videntur parum clari, fiant sollemnes in futurum.

8. Performance for Higher Energy Jets

Lorem ipsum dolor sit amet, consectetuer adipisc ing elit, sed diam nonummy nibh euismod tincidunt ut laoreet dolore magna aliquam erat volutpat. Ut wisi enim ad minim veniam, quis nostrud exerci tation ullamcorper suscipit lobortis nisl ut aliquip ex ea commodo consequat. Duis autem vel eum iriure dolor in hendrerit in vulputate velit esse molestie consequat, vel illum dolore eu feugiat nulla facilisis at vero eros et accumsan et iusto odio dignissim qui blandit praesent luptatum zzril delenit augue duis dolore te feugait nulla facilisi. Nam liber tempor cum soluta nobis eleifend option congue nihil imperdiet doming id quod mazim plac-

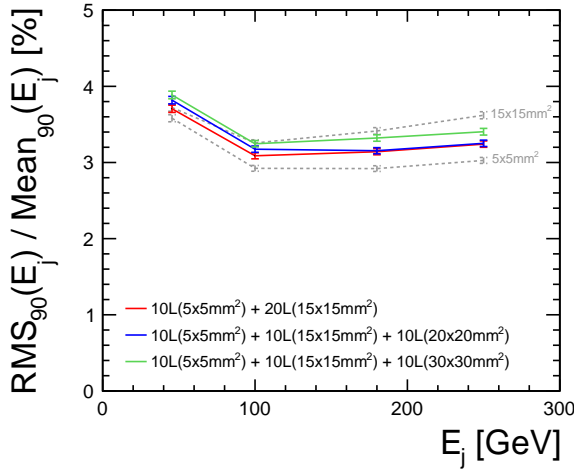
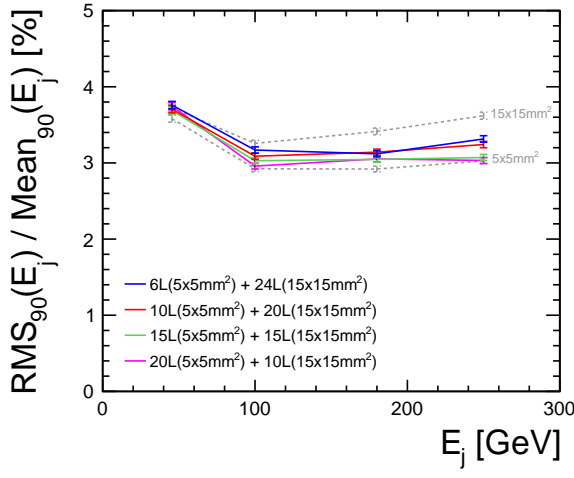


Figure 21

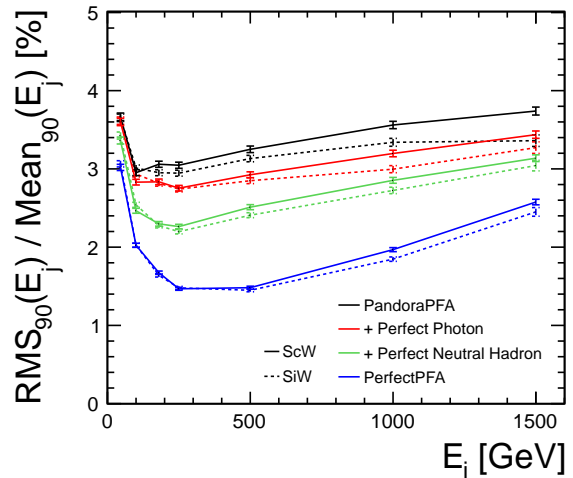


Figure 22

erat facer possim assum. Typi non habent claritatem insitam; est usus legentis in iis qui facit eorum claritatem. Investigationes demonstraverunt lectores legere me lius quod ii legunt saepius. Claritas est etiam processus dynamicus, qui sequitur mutationem consuetudium lectorum. Mirum est notare quam littera gothica, quam nunc putamus parum claram, anteposuerit litterarum formas humanitatis per seacula quarta decima et quinta decima. Eodem modo typi, qui nunc nobis videntur parum clari, fiant sollemnes in futurum.

9. Summary

535 Lorem ipsum dolor sit amet, consectetuer adipiscing elit, sed diam nonummy nibh euismod tincidunt ut

537 laoreet dolore magna aliquam erat volutpat. Ut wisi enim ad minim veniam, quis nostrud exerci tation ullamcorper suscipit lobortis nisl ut aliquip ex ea commodo consequat. Duis autem vel eum iriure dolor in hendrerit in vulputate velit esse molestie consequat, vel illum dolore eu feugiat nulla facilisis at vero eros et acumsan et iusto odio dignissim qui blandit praesent luptatum zzril delenit augue duis dolore te feugait nulla facilisi. Nam liber tempor cum soluta nobis eleifend option congue nihil imperdiet doming id quod mazim plac
538 erat facer possim assum. Typi non habent claritatem insitam; est usus legentis in iis qui facit eorum claritatem. Investigationes demonstraverunt lectores legere me lius quod ii legunt saepius. Claritas est etiam processus dy
539
540
541
542
543
544
545
546
547
548
549
550

551 namicus, qui sequitur mutationem consuetudium lecto-
552 rum. Mirum est notare quam littera gothica, quam nunc
553 putamus parum claram, anteposuerit litterarum formas
554 humanitatis per seacula quarta decima et quinta decima.
555 Eodem modo typi, qui nunc nobis videntur parum clari,
556 fiant sollemnes in futurum.

557 **Acknowledgements**

558 Lorem ipsum dolor sit amet, consectetur adipisc-
559 ing elit, sed diam nonummy nibh euismod tincidunt ut
560 laoreet dolore magna aliquam erat volutpat. Ut wisi
561 enim ad minim veniam, quis nostrud exerci tation ul-
562 lamcorper suscipit lobortis nisl ut aliquip ex ea com-
563 modo consequat. Duis autem vel eum iriure dolor in
564 hendrerit in vulputate velit esse molestie consequat, vel
565 illum dolore eu feugiat nulla facilisis at vero eros et ac-
566 cumsan et iusto odio dignissim qui blandit praesent lup-
567 tatum zzril delenit augue duis dolore te feugait nulla fa-
568 cilisi. Nam liber tempor cum soluta nobis eleifend op-
569 tion congue nihil imperdiet doming id quod mazim plac-
570 erat facer possim assum. Typi non habent claritatem in-
571 sitam; est usus legentis in iis qui facit eorum claritatem.
572 Investigationes demonstraverunt lectores legere me lius
573 quod ii legunt saepius. Claritas est etiam processus dy-
574 namicus, qui sequitur mutationem consuetudium lecto-
575 rum. Mirum est notare quam littera gothica, quam nunc
576 putamus parum claram, anteposuerit litterarum formas
577 humanitatis per seacula quarta decima et quinta decima.
578 Eodem modo typi, qui nunc nobis videntur parum clari,
579 fiant sollemnes in futurum.

580 **References**